

Rethinking Programmed I/O for Fast Devices, Cheap Cores, and Coherent Interconnects

Anastasiia Ruzhanskaia
Systems Group, D-INFK, ETH Zürich
Zürich, Switzerland

David Cock
Systems Group, D-INFK, ETH Zürich
Zürich, Switzerland

Pengcheng Xu
Systems Group, D-INFK, ETH Zürich
Zürich, Switzerland

Timothy Roscoe
Systems Group, D-INFK, ETH Zürich
Zürich, Switzerland

Abstract

Conventional wisdom holds that an efficient interface between an OS running on a CPU and a high-bandwidth I/O device should be based on Direct Memory Access (DMA), descriptor rings, and interrupts: DMA offloads transfers from the CPU, descriptor rings provide buffering and queuing, and interrupts facilitate asynchronous interaction between cores and device with a lightweight notification mechanism.

In this paper we question this wisdom in the light of modern hardware and workloads, particularly in cloud servers. Like others before us, we argue that the assumptions that led to this model are obsolete, and in many use-cases use of Programmed I/O (PIO), where the CPU explicitly transfers data and control information to and from a device via loads and stores, actually results in a more efficient system.

However, unlike others to date, we push this idea further and show, in a real implementation, the gains in average *and tail latency* for fine-grained communication achievable using an open cache-coherence protocol which exposes cache transitions to a smart device. We show this using three use-cases: fine-grained RPC-style invocation of functions on an accelerator, offloading of operators in a streaming dataflow engine, and a network interface targeting for serverless functions, comparing our use of coherence with both traditional DMA-style interaction and a highly-optimized implementation using PIO over PCI Express (PCIe).

1 Introduction

Modern interfaces between CPUs and high-performance devices like network interface adaptors (NICs), storage controllers, Graphics Processing Units (GPUs), and other computational accelerators are designed to optimize *throughput*. Built over a PCIe interconnect, *descriptor rings* in main memory hold queues of operations and completions, and the device performs DMA transactions to read and write both descriptors and payload data. This design, along with the underlying PCIe interconnect, trades off latency for small transactions in favor of high throughput for large ones.

In this paper we question this consensus in the light of workloads which depend for performance not on bulk

throughput, but the cumulative latency of small transactions between CPU and device: closely-coupled hardware accelerators for irregular workloads, or data center Remote Procedure Call (RPC) using small messages. We do this in the context of emerging *cache-coherent* peripheral interconnects like CXL.cache 3.0 [18].

The continuing increase in PCIe bandwidth means that, for a given transfer size, the significance of PCIe *latency* (time to first byte) has become more of a concern, leading to many proposals for reducing the overhead of descriptor management (which we survey in [Section 7](#)).

However, we propose a more radical approach, aimed at use-cases where reduced latency is more important than higher maximum throughput: using PIO to Memory-Mapped I/O (MMIO) devices directly, and avoiding DMA, descriptor queues, operation buffering, and interrupts entirely.

We use a real hardware platform which implements a coherent interconnect between a server-class CPU and a large FPGA to investigate the trade-offs between DMA using descriptor rings, PIO directly over a PCIe interconnect, and PIO over a full cache-coherence protocol.

We show that, for small (around 1KiB or less) transfers, PIO posted *writes* over PCIe significantly outperform DMA, although *reads* are less efficient since, unlike writes, they cannot be pipelined and so incur PCIe’s significant round-trip latency penalty. However, a full cache coherence protocol which avoids PCIe significantly outperforms both DMA and PIO over PCIe.

Crucially, not only is median latency considerably lower, but the *tail of the latency curve* is reduced significantly when using PIO over PCIe, and *completely eliminated* using the cache coherence protocol.

We go further, however, and show how a conventional MESI-like coherence protocol can be *exploited in novel ways* by intelligent devices which can interact with an unmodified CPU at the coherence message level. By *relaxing traditional coherence protocol assumptions* (for example, the independence of cache lines), we can achieve dramatically more efficient communication between a CPU and a device.

In the following section, we provide background and motivation for this work, including the factors that led to the descriptor-based DMA model of I/O, and why it is time to

question the underlying assumptions in that model. In [Section 3](#) we describe and motivate the experimental hardware platform we use for our evaluation, and also provide calibrating performance comparisons with PC data center servers. We show how to use PIO with PCIe in [Section 4](#).

In [Section 5](#), we discuss why true cache-coherent device interconnects are fundamentally different from today’s PCIe platforms, and present a set of efficient protocols for passing messages with low latency between software running on an unmodified CPU, and a smart device which has low-level access to the coherence protocol. In [Section 5](#), we go on to present the implementation of some of these protocols on our experimental platform.

[Section 6](#) then compares a traditional DMA-based approach with PIO over PCIe and our new coherence-based protocols using three different use-cases: (1) lightweight, synchronous local invocation of functionality on a computational accelerator, (2) I/O to and from an intelligent network interface, and (3) hardware offload of a distributed dataflow stream processor to an FPGA. We survey related work in [Section 7](#) and conclude with [Section 8](#).

2 Background and Motivation

Our work in this paper is motivated by the interaction between modern trends in platform interconnect and also the changing ways in which these interconnects are used, particularly in data center and cloud servers.

Interconnects and devices: In early machines, the CPU interacted with peripheral devices exclusively using *programmed I/O* (PIO): the device exposed hardware registers mapped into the processor’s address space. Both data transfer and control of the device involved reads and writes by the CPU to these registers. This model is also known as *memory-mapped I/O* (MMIO).

This model made sense when devices were extremely simple, particularly when augmented by the use of device interrupts to obviate the need for the CPU to poll status registers on the device waiting for an I/O operation to complete. However, the model still requires a synchronous rendezvous between the CPU and device, and moreover requires all data to be transferred via CPU registers (since the CPU is copying data between device registers and main memory).

DMA removes this limitation by allowing the device itself or a dedicated DMA controller to copy the data while the CPU continues to execute other code, providing parallelism and partly decoupling the CPU and device. Further decoupling is provided by *descriptor rings*: producer/consumer buffers of I/O requests in memory represented as a queue of operations, and read and written by both the CPU and the DMA-capable device. In this case, interrupts need only be used when the queue of descriptors becomes full or empty.

Almost every high-speed device today uses essentially this technique, with minor variations such as how the descriptor

queues are formatted, where they are stored, and whether the head and tail of the queue is identified by registers or flags in the descriptors themselves. This model is optimized for throughput – it is most efficient when a large volume of data must be transferred. On modern PCIe interconnects, this consensus results in impressive bandwidth for applications which transfer data in large chunks, up to 64GiB/s for PCIe 5.0 x16.

Surprisingly, increasing state-of-the-art PCIe throughput over time has not been accompanied by a corresponding reduction in *latency*, which has remained a roughly $1\mu\text{s}$ for an interconnect round-trip message exchange [[25](#)].

For the large batch transfers used in GPU-derived programming models (e.g., machine learning workloads), this latency penalty is insignificant when amortized over a large transfer. Indeed, such software has arguably adapted to this model imposed by the hardware [[24](#)].

Recent trends in accelerator design, however, have led to proposed standards for *cache coherent* peripheral interconnects, and the related idea of extending processor cache coherence to heterogeneous devices: accelerators, networking interfaces, and storage controllers [[5](#), [12](#), [18](#), [45](#), [51](#)]. The more far-reaching of these proposals are fully *symmetric*, i.e. devices are first-class participants in a distributed directory-based cache coherence protocol.

Fine-grained workloads: While throughput-oriented workloads involving data transfer between devices and cores (e.g., AI training and inference) are hugely important today, we step back in this paper and consider other workloads that might be a poor fit today for this model, because they involve fine-grained, frequent interaction between the CPU and another device. Many irregular workloads have this property [[7](#), [22](#), [34](#), [58](#)].

Moreover, data center messaging (essentially, RPCs) exchange many small messages [[33](#), [37](#)]. While end-to-end latency is mostly network propagation time in this case, latency incurred in the end system is a good proxy for key resources (such as CPU cycles) wasted before invoking the application code, and in marshaling and sending any reply.

All these workloads incur a significant latency penalty when using DMA for data transfer. Moreover, the assumptions which led to the common DMA descriptor-based model do not hold for these workloads.

For example, CPU execution and I/O were decoupled using descriptor rings because CPU cycles were precious (there being few cores), and the CPU had plenty of different tasks to work on at any time.

This is no longer true. Server CPUs now have 10s or 100s of cores, and moreover when running data center applications they are often dedicated to a single application, sometimes with miscellaneous functions moved to a small subset of the cores [[39](#)]. Most of the CPU cores have nothing to do except handle small messages coming from the network.

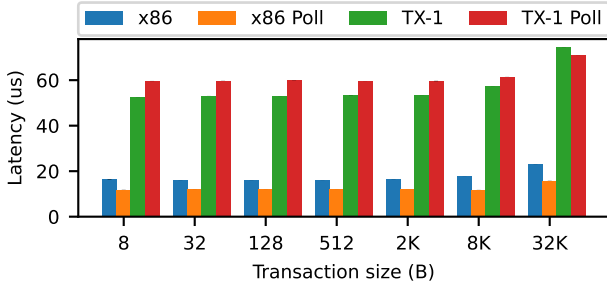


Figure 1. XDMA invocation latency comparison.

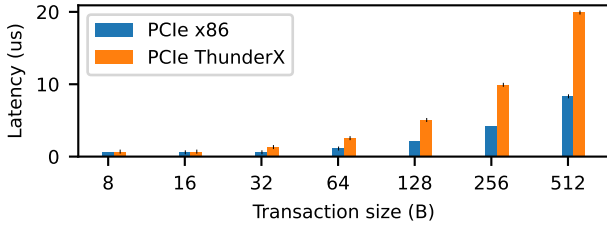


Figure 2. PIO invocation latency comparison.

As a second example: for throughput-oriented workloads DMA has evolved to efficiently transfer data to and from main memory without polluting the CPU cache. However, for small, fine-grained interactions, it is important that almost all the data gets into the right CPU cache as quickly as possible.

These reasons led us to rethink the DMA-based model, and whether directly involving the CPU in data transfers to and from devices might be a better approach for these scenarios on modern hardware. We are not the first to suggest this direction for some cases [13, 36], but we push the question much further: given a future cache-coherent interconnect, what *new ways of using Programmed I/O* might become compelling for data center applications?

Note that we are not proposing abandoning the traditional model, or some of its enhancements we survey in Section 7, for throughput-oriented applications, which can continue to ride the current hardware curve for bandwidth. Instead, we argue it is time to examine complementary alternatives.

3 Experimental platform

We investigate the modern trade-offs between PIO, DMA, and cache-coherent interconnects using a real hardware platform rather than a simulator. Simulation would be appropriate for detailed quantitative comparisons of known techniques, but in this paper we explore unconventional uses of cache coherence and so want to establish not only that our techniques are performant, but that they can practically be implemented in a real system.

The Enzian research computer [15] can be thought of as a two-socket NUMA server, where one socket houses a Marvel Cavium ThunderX-1 CPU, with a Xilinx XCVU9P Field Programmable Gate Array (FPGA) in the other. The CPU is a 48-core ARMv8 processor running at 2.0GHz, and 128GiB of 2133MT/s DDR4 memory spread across 4 memory controllers. Each core has a 32KiB, 32-way associative, write-through, physically indexed, physically tagged, L1 data cache. These are connected to a 16MiB, write-back, 16-way associative, shared L2 last-level cache. Hardware keeps the L1 caches coherent with the L2, and so in ARM architecture parlance the point of coherence is the L1 cache, whereas the point of unification is the L2 cache write-through. The cache-line size is 128 bytes – note that this is double the conventional 64-byte line size.

The CPU and FPGA are connected by the CPU’s native inter-socket cache coherent protocol, the Enzian Coherence Interface (ECI), which Enzian implements on the FPGA. It is a MOESI-like directory protocol with the physical address space statically partitioned between the NUMA nodes (CPU and FPGA). It uses 24 bidirectional lanes (organized into 2 12-lane links), each running at about 10Gb/s, for a theoretical inter-socket bandwidth of about 30GiB/s.

Both nodes have PCIe interfaces: the ThunderX-1 has a PCIe Gen.3 x8 interface, while the FPGA has a PCIe Gen.3 x16 interface. In this work we connect these two interfaces with a loopback cable; this essentially replicates the case of an PCIe accelerator card and allows us to compare PCIe with ECI in our experiments.

While Enzian provides a real hardware platform with server-class performance, direct comparison with modern server platforms is not straightforward: the latter do not offer full cache coherence between CPU and devices, but have more recent, faster cores, memory systems, and PCIe.

We therefore calibrate against a modern PC for both PIO and DMA over PCIe with benchmark comparisons of Enzian and a modern PC (Intel Core i7-7700 3.6GHz Kaby Lake, PCIe Gen.3 x16) with 64-byte cache lines connected to an AMD Virtex UltraScale+ VCU118 card, using the “write then read” experiment detailed in Section 6.1. The VCU118 uses the same FPGA as Enzian, albeit a slightly slower speed gauge.

DMA performance over PCIe: The first experiment uses the Xilinx XDMA IP and its descriptor-based protocol to transfer data between CPU and FPGA over PCIe. Figure 1 shows results for various data transfer sizes, running the Xilinx driver in both interrupt-driven and polled modes.

We see that XDMA over PCIe is about 3 times faster on the PC than on Enzian, while the difference between interrupt-driven and polling performance is much insignificant. Single transaction latency is almost constant on both platforms up to the PCIe transaction size limit of 4KiB, and then increases.

The performance difference between the machines is due to several factors. For small transfers, the CPU overhead of

```

// map 4KiB of PCIe memory for read/write
int fd = open("/sys/bus/pci/devices/.../resource0",
             O_RDWR);
void *pcie_bar = mmap(NULL, 4096,
                     PROT_READ | PROT_WRITE, MAP_SHARED, fd, 0);

// write arguments to PCIe memory
*(volatile invoke_args_t *)pcie_bar = invoke_args;
__sync_synchronize();

// read result from PCIe memory
invoke_res_t invoke_res = *(volatile invoke_res_t *)pcie_bar;
__sync_synchronize();

```

Figure 3. An invocation using PIO & PCIe. Error handling omitted.

descriptor setup dominates, and an x86 core is simply faster than a ThunderX-1 core. In addition, the memory system is somewhat faster on the PC. The factor of 2 difference in PCIe *bandwidth* between the two platforms does not appear to be a factor in these experiments.

PIO performance over PCIe. In the second calibration experiment the CPU performs PIO reads and writes over PCIe to the FPGA. We experimented with several different optimizations in this experiment (see Section 4), in particular the use of write combining and vector instructions. We present the best figures obtainable on each platform.

Figure 2 shows that for transaction sizes above 32 bytes, the PC is about twice as fast as Enzian over the PCIe cable between CPU and FPGA. Here, the difference in PCIe bandwidth is responsible for the latency difference, in particular for reads (limited to 128 bits on both platforms). Writes, in contrast, are combined and pipelined at the PCIe interface.

4 Programmed I/O over PCIe

PCIe is complex, and we spent considerable time optimizing CPU-initiated reads and writes for different platforms. We describe here how we arrived at optimally-efficient PIO latency to the FPGA over PCIe.

We pre-map PCIe apertures (BARs) into user space on the CPU and measure latency as the time to write a value to this space (thereby *invoking* a function on the device) and read a result back (Figure 3).

PCIe memory writes are *posted* transactions and may complete out-of-order, allowing multiple requests in-flight at the same time. Most systems also have dedicated bus units to combine writes and coalesce transactions. Enzian’s ThunderX-1 performs *write-combining* for stores to PCIe, allowing 512 bits per bus round-trip (confirmed with a logic analyzer) and resulting in efficient PIO write transactions.

In comparison, PIO reads over PCIe show low latency for small data but degrade quickly as size increases. This is because PCIe memory reads are *non-posted*, forcing each read to finish before the next can start and incurring a round-trip

time cost (about $1\mu\text{s}$) for each word. Many systems also have a narrow read bus between CPU and PCIe; the ThunderX-1 peripheral access bus is only 128 bits wide.

This means that on ThunderX-1, common optimization techniques like vector instructions have negligible benefit for PIO over PCIe: the hardware already coalesces writes into 512-bit transactions and reads are limited by the read bus width of 128 bits.

x86 has more optimization opportunities for PIO reads and writes. The Intel Data Streaming Accelerator [28] offers `MOVDIR64B` and `ENQCMD` instructions, allowing 64-byte PIO writes with *write-combining* mappings and user-space descriptor submission without driver intervention. Mapping memory with *write-through* attributes, as suggested by Tide [26], allows cache line-sized PIO reads. These architecture-specific extensions are not available on ThunderX-1.

5 PIO over a coherent interconnect

We now turn to programmed I/O over a cache coherent interconnect. A naive approach would have the CPU simply copy data over a coherent interconnect as in conventional PIO. This requires careful cache management on the CPU using explicit cache flush and invalidate instructions, but is appropriate when the hardware standard mandates a cache on the device, as with OpenCAPI 4.0 [2, 51].

However, we are more interested in how a coherent interconnect can best perform low-latency, efficient data movement between CPU registers and device hardware, *including* cases where the conventional notion of the cache as a view over memory contents is not appropriate, such as data arriving over a network.

Scoping: We scope the scenario further to the case where the CPU cores, or their Last-Level Cache (LLC), communicate with devices via a MESI-like [43], message-based coherence protocol with stable states corresponding to `MODIFIED` (dirty), `SHARED` (clean), `EXCLUSIVE` (clean), and `INVALID`, using a distributed cache directory. Note that this means that each address or cache line has a *home node*, which maintains the directory entry for the line.

We also assume a *symmetric* protocol: each device is a first-class participant in the protocol with a subset of physical addresses homed at it, and the device therefore maintains directory state for these lines (although it might not actually cache data itself). Moreover, we take the perspective of the device designer: the *device sees individual cache messages*, rather than transparently coherent memory.

These assumptions are rare in hardware today but they do hold for proposed standards like CXL 3.0 [18], and also for the Enzian platform we use in experiments.

Baseline: simple coherence. We first discuss using simple cache coherence to re-apply existing techniques *inter-core*

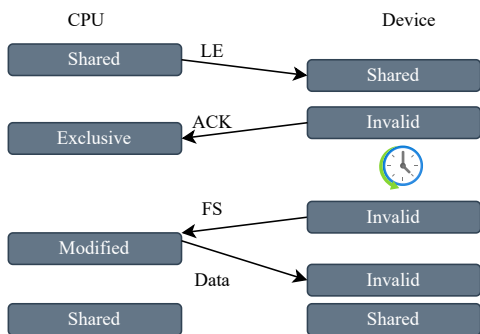


Figure 4. Simple inter-core communication over coherence

communication in software, such as FastForward [20]. Here (Figure 4), the sender (CPU) writes data to a cache line on which the receiver is spinning reading. Assume the line starts in SHARED state in both caches. When the sender writes the line (typically atomically via the core’s write buffer), it transitions briefly to MODIFIED state, before being fetched by the receiver over the interconnect and reverting to SHARED.

This can be highly efficient in software, particularly when deployed as a ring buffer of cache lines, and results in minimal interconnect traffic (since the receiver spins on a local copy of the line), although the CPU itself must spin. Indeed, this is the technique recently used in CC-NIC [49] to emulate a NIC using a different CPU socket.

However, this design assumes that each endpoint can only manipulate its local cache using software instructions (loads, stores, etc.) and also that flush or invalidate instructions should be avoided for performance reasons. This is not the case when one of the endpoints is a device with message-level access to the cache coherence protocol, and possibly maintaining its own directory state.

The implications of message-level access. A device on a symmetric coherent interconnect can see more cache state and events, and also initiate more operations, than a CPU core can. Note that this does not entail a cache *per se* on the device at all, indeed this is rarely appropriate.

First, the device **receives messages** from the CPU cache that request lines in SHARED or EXCLUSIVE state, or which request that the caching state on the device be downgraded (e.g., from EXCLUSIVE to SHARED, or from SHARED to INVALID). It is free to react internally to these events as it chooses, as long as it does not violate the protocol.

Second, the device can **issue such requests** itself at any time, allowing more fine-grained control of the state of a line in the CPU’s cache.

Third, for lines which are homed at the device, the device’s directory maintains explicit **information about the cache line state** at the CPU and other nodes as well as locally.

Fourth, unlike a conventional cache, the device **does not have to respond immediately** to every request from the CPU’s cache. Instead, it can choose to delay the response (blocking the requesting core) until some other operations complete. Care must be taken to respond before any hardware-imposed timeouts, but these are typically generous (hundreds of milliseconds on the ThunderX-1, for example) and can be worked around in software (e.g., by sending a “try again” response within the timeout).

Finally, the device can **choose to interpret events** like remote requests as more than simply loads or stores to the line concerned. This last insight is important because it, in combination with the previous observation, it allows us to construct efficient communication mechanisms which rely on a combination of the device’s richer view of the protocol and the software on the CPU adhering to additional conventions to communicate channel semantics to the device.

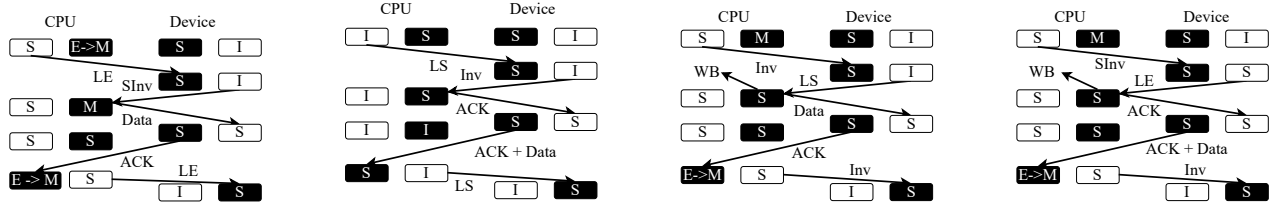
Put simply, requests to specific cache lines can be used to signal particular higher-level operations to the device, much as register reads and writes to traditional devices frequently have semantics very different from memory access.

This is an oversimplification, and we discuss the subtleties that arise below. First, however, we present four related communication protocols, layered above MESI-like coherence, which provide for efficient, blocking communication between a conventional CPU and a coherence-aware device.

Communication protocol design variants. We present 4 different but similar communication protocols (shown in Figure 5) which vary based on whether (a) the CPU or the device initiates the message transfer, and (b) the cache lines used are homed on the CPU or device. All provide a synchronous invocation: a transfer of a single cache-line-sized message, followed by a single cache-line response. All use 2 cache lines, which we designate A and B. These protocols can be generalized to larger payloads, and latency will grow linearly with the payload size. Interestingly, they can be made slightly more efficient by using more cache lines, but quickly become complex. We focus on the simple 2-line case in this paper.

The protocols use the same techniques and insights, and are best described using the example of a CPU-initiated invocation on the accelerator using addresses homed on the device (Figure 5a). An implementation of this protocol is used for the evaluation in Section 6.1. Note that, unlike RPC, invocations are local to the machine and avoid marshaling or unmarshaling of messages.

1. The protocol starts with line B in EXCLUSIVE state in the CPU cache, and line A INVALID (we show how this can be conveniently achieved below). To initiate an operation, the CPU writes the request data from its registers into line B, which transitions to MODIFIED. This happens without communication with the device, since B was previously in EXCLUSIVE.



(a) CPU-initiated, device-homed (b) Device-initiated and homed (c) CPU-initiated, CPU-homed (d) Dev.-initiated, CPU-homed

Figure 5. Protocol variants for efficient CPU-device messaging

- To signal to the device that line B holds a new request, the CPU then executes a load to line A. Since A is INVALID, the cache requests A in SHARED from the device. This violates the typical convention that cache line operations are independent, but the device is free to interpret this request for A as a signal from the CPU that B holds a request.
- The device *does not respond* immediately to the request for A, thereby stalling the load and blocking the requesting core. Instead, it requests B from the CPU’s cache, in EXCLUSIVE. The interconnect therefore transfers the request data to the device, and line B duly transitions to INVALID in the CPU’s cache.
- The device reads the data it has received in B, and computes a result on it, which is to be returned to the CPU. It returns this using the response to the CPU’s request for cache line A.
- The CPU cache receives line A’s new data and the CPU unblocks, immediately loading the first word of the invocation response into a register.

As described, the end state is that A is now INVALID and B is SHARED in the CPU cache. However, in some deployed MESI-like protocols (including the Enzian interconnect we use), the device is free to return the data stipulating that it is not SHARED but now EXCLUSIVE to the CPU. This final feature leaves the cache in the state it started in, with the roles of A and B reversed, ready for the next transaction.

The whole exchange takes 2 round trips on the coherent interconnect, and require no spinning on the CPU.

The other 3 protocols work similarly. For example, Figure 5b shows the analogous case where the device initiates the request to the CPU, but still using lines homed on the device. This is used for the NIC experiment in Section 6.3.

The remaining two cases, where the cache lines are homed on the CPU, are more complex to deal with, since there is a possibility that the CPU cache will evict one of the cache lines without warning. The device will not observe this, and so might incur an access to main memory on the CPU node. In this paper we therefore focus on the case where the cache lines are homed on the device.

Subtleties: A number of issues must be handled to make this practical, starting with timeouts: we block a core’s request for a cache line until a device operation has completed. A timeout in the CPU’s cache is likely to cause a memory fault exception, a fatal machine check, or the processor simply locking up (on Enzian, it is a machine check).

We solve this issue with a small state machine on the device that returns a “not ready yet” response before an impending timeout, causing the software on the issue another request for the other cache line, extending the response time indefinitely without the need for spinning. In practice, we target operations that are shorter than the timeout.

The second issue concerns deadlock due to the device stalling a request until it can issue, and get a reply back for, another request to a different cache line. Existing standards for interoperable cache coherent interconnects are silent on what happens in this situation, possibly because it has not occurred until now. The design assumes that transactions on different cache lines can progress independently.

In most implementations, this assumption typically holds in order to maximize the memory bandwidth utilization and minimize request latency, and also to simplify reasoning about deadlock freedom of the coherence protocol itself. However, it may be the case that the cache stripes transactions across a limited number of independent units and which might deadlock if both A and B were mapped to the same unit. Were this to be the case, it could be avoided by careful placement of A and B in the physical address space. This is actually the case in our FPGA device implementation, described in Section 5.

Implementation in Enzian. We implemented the two device-homed protocols over Enzian and evaluate them in Section 6. The implementations use SystemVerilog and SpinalHDL [16] and exploit an existing “Directory Controller” on Enzian’s FPGA [47] which manages the coherent links to the CPU and handles transient states in the ECI protocol.

ECI provides all the messages we require to implement our messaging protocols. In particular, it includes the ability for the device to return a line to the CPU cache in EXCLUSIVE state, even though the CPU requested it in SHARED.

This optimization dramatically reduces latency, as shown in Section 6.1.

In our case, no flow-control issues arise since ECI uses separate virtual channels for request and reply messages, removing the chance of deadlock. However, other complications arise: ThunderX-1 generates Global Synchronization (GSYNC) messages which function as global barriers. A GSYNC blocks any subsequent transactions until all those started before the GSYNC have retired. Fortunately, any invalidations sent are not blocked by core, allowing the protocol to progress regardless.

The ThunderX-1 divides its last-level cache functionality into a set of units called TADs, each of which can handle up to 16 simultaneous cache transactions. We ensure that consecutive cache lines are mapped to different TADs to ensure that the operations can proceed independently.

The ARMv8-A weak memory model means that barriers are needed to reliably order reads and writes. For example, it is critical that the core’s write buffer is drained into L1 cache (which is write-through to the L2) before a subsequent load from the core signals to the FPGA that the line can be pulled, and this requires a DMB barrier instruction between the writes and the read. On the ThunderX-1 this is sufficient to ensure ordering observed at the FPGA.

6 Evaluation

We compare PIO over a coherent interconnect with two other reference points: PIO directly over PCIe – essentially, the CPU copying data to and from a region of PCIe address space – and descriptor-based DMA over PCIe. All use the same Enzian hardware platform. Coherent PIO uses the Enzian native ECI, while the two PCIe techniques connect the CPU and FPGA PCIe interfaces back-to-back with a loopback cable as described in Section 3, effectively turning the Enzian FPGA into a conventional PCIe FPGA card. DMA experiments all use the Xilinx XDMA hardware IP on the FPGA.

We explore three different application scenarios: synchronous invocation to an accelerator on the FPGA, a closely-coupled high-speed NIC, and a stream processor which moves some of its dataflow operator graph to the FPGA.

6.1 Invoking functions on an accelerator

We first measure latency when the CPU invokes a function on the device, passing arguments, and obtaining a result. We use the protocol shown in Figure 5a, whereby the cache lines are homed on the FPGA.

Figure 6 shows the distribution of total latency for the this operation. We see a median latency of around 1600ns for the *unoptimized* protocol, wherein the result line is returned in SHARED state as it was requested by the CPU. When we introduce the optimization of returning the line in EXCLUSIVE, the median latency drops to around 900ns.

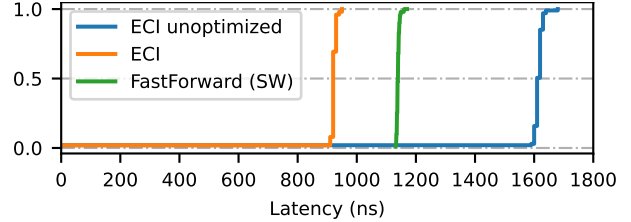


Figure 6. Invocation latency over ECI vs. FastForward

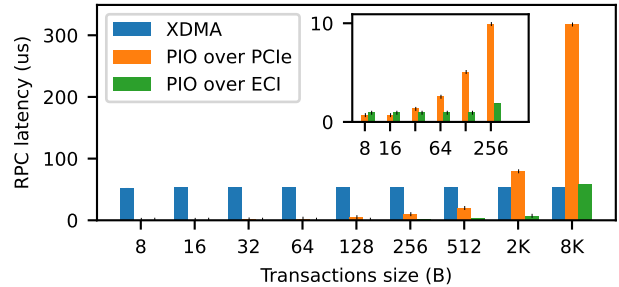


Figure 7. Invocation latency for different payload sizes

For comparison, we also show an implementation of the FastForward protocol [20] exchanging cache lines between CPU sockets in a dual-socket ThunderX-1-based Gigabyte R150-T61 server with similar CPU and DDR specification to Enzian; this achieves a median latency of about 1150ns.

The optimized protocol is performing 2 round-trip message exchanges over ECI, which has a one-way latency at the link layer of about 150ns. The rest of the overhead (300ns) is mostly incurred in the protocol processing in the directory controller. The FPGA is clocked at about 300MHz.

A significant penalty is incurred when the results of the call are returned in SHARED, resulting in further round trips over ECI to (unnecessarily) invalidate the line at the FPGA before sending the next message. This suggests that future coherent interconnects would benefit greatly from allowing the home node to return a line in EXCLUSIVE.

Overall, the optimized protocol comfortably outperforms FastForward, despite the latter exploiting highly optimized hardware implementations at both ends (clocked at 2.1GHz) and aggressively polling, whereas our optimized protocol requires no spinning on the part of the CPU or device.

6.2 Invocation over ECI vs. PCIe PIO and DMA

We now compare the latency achieved in the previous section with both PIO over PCIe and the Xilinx XDMA hardware using descriptors. For DMA numbers we use the Xilinx XDMA benchmark [57], which essentially performs the same operation using descriptor-based DMA. In both these cases, the FPGA is configured to map the request and response into a write to, and a read from, onboard Block RAM.

As in Section 6.1, we measure latency to send a request from the CPU to the FPGA and read a response. However, this time we vary the payload size (of both request and response) and report median latency figures.

The results are shown in Figure 7. Up to payloads of 8KiB, the latency of XMDA-based communication is dominated by descriptor setup and manipulation, and remains largely independent of payload size. Faster PCIe interconnects (this is a PCIe Gen3 x8 link) would amplify this effect.

Latency over ECI is dramatically lower for smaller payloads. Unsurprisingly, it is constant up to 128 bytes (the size of a cache line on Enzian) and then increases linearly, since the protocol simply replicates each cache line exchange until all the data has been transferred. It is only at 8KiB that ECI invocation latency exceeds that of XMDA. Arguably the transfer of multiple cache lines over ECI might be improved by clever pipelining and locating the lines in physical memory so as to exploit parallelism in the directory controllers, but we do not explore that in this paper.

Relative to ECI, PIO over PCIe performs poorly except for payloads under 16 bytes in size. This is due to limitations in PCIe that we have discussed in Section 4, notably the limited read bus width.

We conclude that up to the page size (4KiB) or the typical size of jumbo frames, PIO remains significantly faster than the DMA option commonly used for these transaction sizes. Thus even using the XDMA implementation for the experiments we still have the room for comparison with optimized DMA implementations.

This experiment is closed-loop and single-threaded, and so achieved *throughput* is proportional to the round-trip latency. Fully saturating the raw link bandwidth (in all cases) would require many parallel invocations at once, which would go against our goal of supporting applications where latency is paramount.

6.3 Network interface adapter

We now compare the different approaches in the context of data center networking. It is common to see very low latency figures ($< 1\mu\text{s}$) in data center packet switching and delivery [21, 23, 31], motivating the need to minimize latency between the network itself and CPU registers [19].

We implement 3 variations of a 100 Gb/s NIC in Enzian. The first (Figure 8a) is a conventional approach connecting one of Enzian’s 100 Gb/s Ethernet MACs directly to the XDMA engines, resulting in a NIC programmed using descriptor rings. The second design (Figure 8b) buffers packets in onboard SRAM on the FPGA and allows the CPU to read and write packet and control data using PCIe reads and writes. The final approach (Figure 8c) uses a custom module on the FPGA to bridge between the ECI directory controller and the Ethernet MAC, using a slight variant of the protocol

Table 1. NIC implementations: latency percentiles on selected packet sizes. Higher tail latencies are marked in **bold**.

Size	Percentiles RX (μs)				Percentiles TX (μs)			
	P50	P95	P99	P100	P50	P95	P99	P100
PCIe DMA								
64	65.39	66.36	67.65	100.01	10.06	10.35	10.59	16.49
1536	64.77	65.59	66.21	133.84	10.89	11.12	11.33	30.84
9600	65.89	67.12	68.05	123.61	15.73	16.05	16.29	41.99
PCIe PIO								
64	3.25	3.26	3.27	3.39	0.34	0.36	0.38	4.80
1536	72.89	72.93	72.96	73.05	1.82	1.84	1.86	6.40
9600	450.28	450.35	450.38	451.10	9.91	10.01	10.07	10.14
ECI PIO								
64	1.05	1.06	1.07	1.17	1.06	1.12	1.14	1.18
1536	7.24	7.29	7.39	7.43	3.09	3.26	3.50	3.59
9600	39.43	39.48	39.50	39.55	9.07	9.19	9.65	9.95

in Figure 5b to deliver network packets to the CPU in multiple cache lines. In all cases we clock the core NIC logic at 250 MHz.

For experiments we configure the Ethernet MAC in near-end PCS/PMA loopback mode for a reliable measurement of packet delivery *inside* the server without network delays. We define the receive latency as time passed from the last beat of the packet appearing on the ingress streaming interface of the Ethernet MAC, to the CPU fully receiving the packet content in its registers. The transmit latency is defined similarly as time passed from the CPU having the packet ready in registers, to the last beat of the packet appearing on the egress streaming interface on the MAC. We do not include the time it takes the packet to go through the Ethernet PCS/PMA loopback, since the MAC is fixed and the same in all implementations presented in this experiment.

To minimize disruptions from the Linux scheduler, we follow the common practice to free one CPU core from kernel tasks and IRQ processing [1], with the `isolcpus` function together with core pinning using `taskset`. In this setup, the only disturbance from Linux would be the 250 Hz timer interrupt present on all cores. While a custom, completely *tickless* kernel would remove this disturbance completely, it is not commonly deployed in production environments due to performance complications. We use such a tickless kernel to measure tail latency below, but other experiments use a stock generic kernel from Ubuntu.

We show figures for XDMA in both polled and interrupt-driven modes; in practice the difference in latency is small.

Figure 9 shows receive latency for different packet sizes for each of the NIC implementations. As in the invocation experiment, DMA latency is fairly stable across all packet sizes, suggesting that the latency is dominated by various DMA overheads, such as descriptor setup and manipulation.

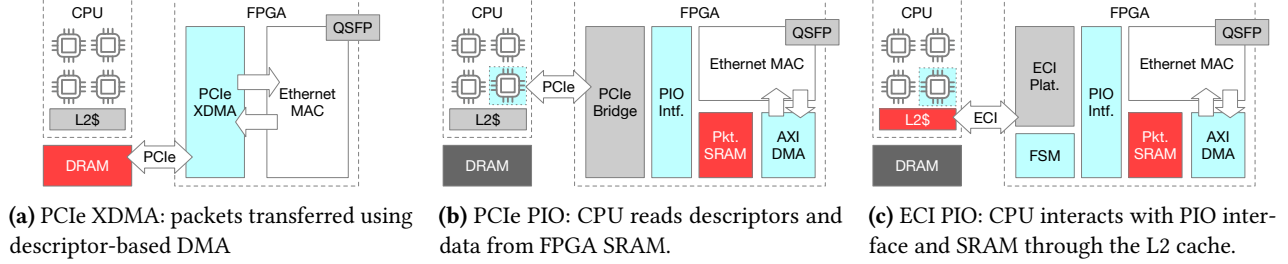


Figure 8. Different NIC architectures. Blue denotes data movers; red denotes memory that holds packet data.

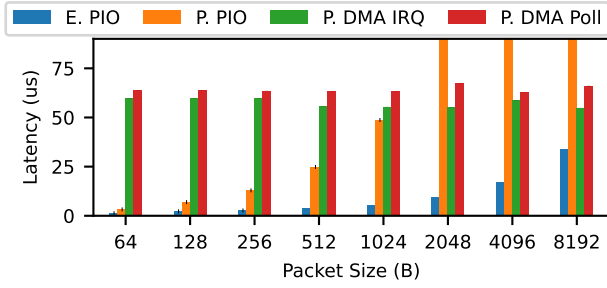


Figure 9. NIC implementations: receive latency

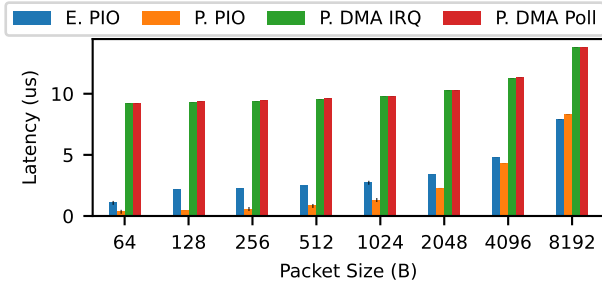


Figure 10. NIC implementations: transmit latency

Note that system calls here actually result in little overhead (only a few μs); the overhead is dominated by cache misses manipulating DMA data structures in main memory.

In contrast, PIO over both ECI and PCIe offer much lower latency for small packet sizes up to 1024 bytes DMA, highlighting high efficiency gains in PIO compared to DMA. However, the latency of PCIe PIO quickly degrades for larger packets due to the *non-posted read* problem discussed in Section 4, reaching over 350 μs for 8 KiB packets. In contrast, ECI offers dramatically better latency even at 8 KiB packets.

Figure 10 shows transmit latency. In this case, PCIe PIO competes well with ECI across all packet sizes due to combining posted writes as we discussed in Section 4. PIO over ECI shows a slightly higher latency for small packets, due

to it needing 2 round-trips over ECI for each 128 bytes, versus a single PCIe round trip. Both PIO solutions perform significantly better than DMA across all packet sizes.

Table 1 shows the tail latency impact for selected packet sizes for each of the NIC implementations. We select three representative packet sizes to evaluate tail latency: 64 for the smallest possible packet, 1536 for the normal Ethernet MTU, and 9600 for a common jumbo frame MTU. We use the *tickless* kernel setup mentioned earlier to avoid the 250 Hz Linux timer, in order to reveal the actual tail latency impact from our NIC.

We see that PIO over PCIe results in low tail latency compared to the descriptor-based approach, while ECI *completely eliminates* tail latency in this scenario.

These results show a clear advantage of using PIO over DMA, even for larger packets, and especially when using a coherent interconnect. The poor receive performance of PCIe-based PIO for receiving packets is due to the unposted-read limitation of PCIe, and disappears for transmit.

6.4 Accelerating Timely Dataflow

In this example we apply the techniques and results outlined so far to a practical workload: Timely Dataflow [42], a real-time stream-processing system. We compare the baseline performance to a partially FPGA-offloaded implementation under three CPU-FPGA communication scenarios: DMA over PCIe, PIO over PCIe, and PIO over ECI.

Timely Dataflow schedules operators in a user-defined dataflow graph to evaluate complex operations on large streams of data, operating on variable-sized batches. Operators may be arbitrarily complex and are independent, and thus benefit from offloading where the overhead of shipping the data to the FPGA is compensated by greater throughput of the offloaded operators.

To test the limits, we construct a worst-case scenario: a large (31-element) graph of simple operators (filters). The large graph maximizes communication overhead in the form of progress tracking data, while the simple operators leave the FPGA with only a small performance lead over the CPU. We want to predict whether PIO can make FPGA offload work in regimes where the fixed overheads of DMA make it

impractical, for example where small batch sizes are needed to ensure data freshness (as in Differential Dataflow [40]).

The first (blue) bars of Figure 11 show the baseline performance of the non-offloaded (CPU-only) system against batch size. Note that the horizontal axis is a log scale; All four curves are actually straight lines, with offsets and slopes obtained by a least-squares fit listed in Table 2 along with the coefficient of determination (r^2). The remaining bars cover the three offload cases. Each is the median of 1000 samples.

While no offload configuration beats the baseline, the two PIO cases outperform DMA up to batch sizes of 512B (for PCIe) and 4KiB (for ECI), with ECI almost matching the baseline at the smallest batch size (128B). To understand why offloading fails to produce a speedup in this example, and what changes will be necessary to allow it to, we look more closely at the fitted coefficients in Table 2.

As shown by the r^2 values, the fit for each dataset is excellent. We can thus model the time taken to process a batch as a fixed component, or overhead, independent of the amount of data processed (e.g., running the Timely scheduler, or setting up DMA descriptors) plus a component which scales linearly with the size of the batch.

Compared to the baseline, DMA offload has a significantly lower per-byte cost (3.7 vs. $8.7ns/B$) but higher fixed cost ($336\mu s$ vs. $204\mu s$). This includes the cost of descriptor setup and interrupt handling, while the per-byte cost shows the higher throughput of the FPGA. This includes both computation and data transfer but as DMA makes very efficient use of the (PCIe 3.0 x8) interconnect, once setup costs are paid, the per-byte transfer cost is on the order of $0.1ns$, allowing us to estimate the per-byte cost of FPGA compute at $3.6ns/B$. The CPU figure represents only compute.

This linear model predicts a break-even at 26KiB. This matches the observed data (not plotted) where DMA offload first outperforms the baseline at a batch size of 32KiB. Whenever the FPGA compute cost is at least $0.1ns$ lower per byte than the CPU, DMA offload will outperform for large enough batches. However, due to the large fixed overhead it can never outperform the CPU for batches smaller than 16KiB. This limits its usefulness where small batch sizes are needed.

While they make less efficient use of the interconnect bandwidth (as indicated by their higher per-byte costs), their lower fixed overhead allows the PIO modes to significantly outperform DMA at smaller batch sizes. What would it take for the faster of the two (ECI) to outperform the CPU at a moderate batch size?

As the FPGA pipeline is identical in all cases, the limiting factor is the per-byte transfer cost. Taking our above estimate of FPGA compute at $3.6ns/B$, we can estimate this cost at $30 - 3.6 = 26.4ns/B$. Letting S stand for batch size and C for this transfer cost, the two break even where

$$204\mu s + S \times 8.7ns/B = 221\mu s + S \times (C + 3.6ns/B)$$

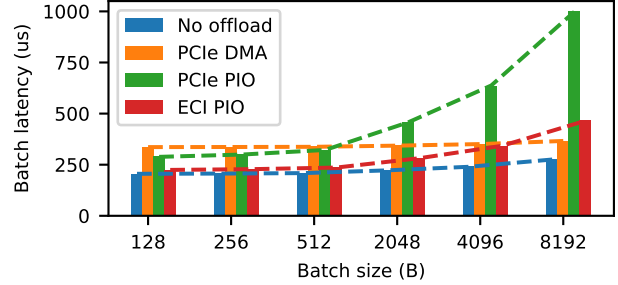


Figure 11. Timely Dataflow offload, graph size 31

Table 2. 1st-order (offset + slope) coefficients fitted to the data series of Figure 11, as cost per byte and fixed overhead

	Time/Byte (ns)	Overhead (μs)	r^2
Baseline	8.7	204	1.00
PCIe-DMA	3.7	336	0.99
PCIe-PIO	88	277	1.00
ECI-PIO	30	221	1.00

Rearranging gives

$$C = 5.1ns/B - 17\mu s/S$$

$5.1ns/B$ being the speedup due to FPGA processing and $17\mu s$ the fixed overhead relative the baseline, the negative sign due to the higher-than-baseline overhead.

From this we see that given the overhead the smallest batch for which a speedup is possible is around 3300B, and that a batch size of 4096B demands a transfer cost not more than $0.95ns/B$, or $120ns$ per 128B cache line. As the existing protocol serializes on each line, this cost includes the round-trip latency. As the hardware can handle many in-flight transfers at once, modifying the protocol to transfer 32 lines at once would reduce the per-byte cost enough that ECI-PIO offload breaks even.

Additionally, bringing the fixed cost down reduces the smallest practical batch. If the relative overhead could be brought below $500ns/batch$ then with parallel cache lines giving a $1ns/B$ transfer cost, FPGA offload using ECI-PIO would outperform the CPU from a batch size of 128B. With such an optimized protocol, ECI-PIO would outperform all other cases until a batch size of 142KiB, above which PCIe-DMA would overtake it.

6.5 Offloading Bloom Filters

In a second acceleration experiment we offloaded Bloom filters [9] to the FPGA. Bloom filters are used to efficiently check whether an element is a member of a set. It uses little memory and allows for fast lookups. A Bloom filter is equipped with k different hash functions and a lookup table. Testing the presence of an element requires computing these

k hash functions and querying the lookup table with the results.

We took inspiration from the applications discussed in Fleet [54]. As the CPU baseline, we re-implemented the Fleet C++ code in Rust as a Timely Dataflow operator. In the Fleet implementation, the hashes were computed in parallel for each byte sequentially using AVX instructions, which we replicated in Rust using SIMD instructions. On the FPGA side, the hash computation is parallelized and the iteration over the element’s bytes is pipelined. We present the numbers of using a single thread on CPU and a single compute unit on FPGA in order to keep the comparison fair.

With the Bloom filter integrated into Timely Dataflow as a single offloaded operator, most of the additional overhead from processing sub-graphs is eliminated and the flow of data between FPGA and CPU is reduced to the minimal practical batch. In addition, the computational load is significantly higher compared to a simple filter. The k hash functions consist of sequential bit shifting, addition, and XOR-ing, which are very fast in FPGA logic and deliver the offloading benefit comes from. Therefore in this application we concentrate on minimal practical batches and direct offloading benefits.

We implement the Bloom filter on the FPGA to take 128-byte elements with $k = 8$ hash functions that take byte-wide inputs. We unroll the hash function calculations for each byte lane by a factor of 2, resulting in a 64-cycle latency for each element. We then pipeline the calculations with an initiation interval of 2 cycles to saturate the 512-bit bus. The return value is the set of 8 64-bit hashes for each element.

Instead of directly returning the hash results, the FPGA could have computed the lookup table positions or performed the lookup itself, returning either k indices or binary values. In the case of indices, the read-to-write ratio would stay the same as in our approach, but for the lookup, the read requests would be minimized and writes would dominate. In this experiment, we assume that the lookup table is located elsewhere and focus on efficiently calculating the hash function and transferring the results to the lookup table.

In Figure 12, the latencies for PIO and CPU both start around $25 \mu\text{s}$, due to the high overhead of streaming the input data. The real processing time of one element is $2.6 \mu\text{s}$ on the CPU and $1.7 \mu\text{s}$ when offloading with ECI. As overall processing time increases with the data size, we see the gap between CPU and PIO more clearly. After 8 KiB, same as in previous experiments, XDMA starts to perform better than other approaches as performance becomes dominated by the higher bulk throughput of PCIe DMA.

7 Related work

Cho *et al.* [14] provide an excellent survey of existing CPU-device communication mechanisms, and address high-speed storage devices with microsecond latencies. They question

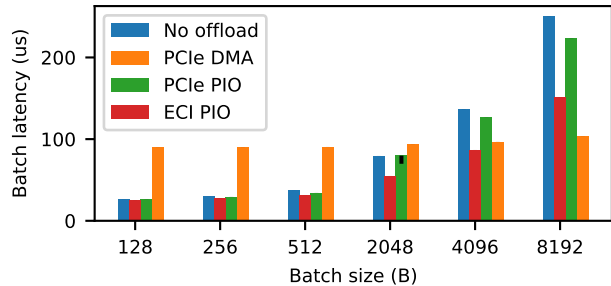


Figure 12. Offloading Bloom filters to the FPGA

the conventional wisdom that *hiding* the latency of interacting with such devices is not possible using existing techniques, and show how access latency using existing descriptor-based protocols can be effectively hidden by clever use of prefetching, better hardware queues, and user-level context switching. Our work is different (and complementary) in reducing the actual latency of each message between CPU registers and device memory.

7.1 Improving descriptor-based DMA

Cohort [55] proposes a single, uniform, single-producer, single-consumer, queue-based DMA descriptor interface to all accelerators on an System-on-Chip (SoC) which replaces the variety of ad-hoc interfaces found on most SoCs. Cohort mandates an MMU on each accelerator, which maintains consistency with CPU MMUs and allows seamless user-space access to accelerator queues, and integrates with the cache coherence protocol to optimize the use of lock-free descriptor queues. We focus instead on what a latency-optimized interface might look like, eschewing descriptors in favor of direct cache line transfers.

Ensō [48] shows the benefits of replacing the packet-based DMA software interface used by modern NICs with one based on a contiguous large buffer of opaque, variable-sized messages, with metadata sent via a different completion buffer. Ensō replaces descriptors with this buffer using an ingenious combination of direct MMIO writes to the PCIe device and polling memory queues written by the NIC. Our work similarly tries to reduce the overhead of descriptor management, but by focusing solely on latency-sensitive small payloads and avoiding DMA access completely.

7.2 Coherent interconnects

Coherent replacements or extensions of existing device interconnects have been under development for some time and are beginning to see widespread availability. IBM’s Open-CAPI [51] builds on PCIe by adding a protocol layer for coherence. It and the competing Gen-Z [35] and CCIX [12] protocols have meanwhile been either merged into or replaced by CXL [38], which seems likely to be the standard

interoperable protocol in the short- to medium-term future. However, commercial CXL hardware implementing the more recent revisions, which allow less restricted use cases, is still not widely available.

Other notable coherent interconnects include the RISC-V-specific TileLink [8, 17, 53] and NVIDIA’s NVLink 2.0 [45, 56]. TileLink is an open standard and suitable for research but hasn’t yet been implemented in server-scale hardware. NVLink is proprietary and closed.

Existing work has built on the available research platforms to explore the design space for practical applications. Centaur [46] demonstrated the FPGA offload of database operations on Intel HARP v1. However, while Intel HARP [27, 29] coupled a CPU and FPGA using a coherent QPI link, it provided a pre-configured coherent cache in the FPGA rather than user access to coherence protocol messages. In contrast, this access is readily available in Enzian [15].

Open, extensible protocols have been used to explore coherent offload in simulation, including making the case for protocol specialization building on the Spandex protocol family [3, 4]. CoNDA [10] likewise employed simulation to explore the design space for coherent device interconnects, with a focus on reducing unnecessary message traffic.

The Denovo protocol [50] is presented as an improvement specifically for CPU-GPU coherence, tailoring the protocol to match the comparatively predictable access patterns of typical GPU workloads.

7.3 Cache line-based communication

Communication in software between peer nodes in a cache-coherent system is typically very different from using descriptor-based DMA. FastForward [20], Barrelfish [6], Concord [30], and Shinjuku [32] adopt a much more direct approach to sending small messages with low latency, e.g., by exploiting the cache coherence protocol to transfer lines between caches on demand, and local polling to provide synchronization. Recently, cache coherence between NUMA CPUs has been used to *simulate* communicating between software and a hypothetical cache-coherent NIC [49].

Other work [52] has already noted that the cache line is a better unit of transfer where small operations are expected, as in FastForward [20] and Barrelfish [6] protocols. More recently Concord [30] communicates scheduling decisions between workers and the dispatcher via a polled cache line, converting worker threads from interrupt-driven to poll-mode “CPU drivers”. A similar technique is used in Shinjuku [32].

A recent study of data center RPC from Google [33] reinforces the importance of small transfers and highlights the large latency of PCIe transactions.

HyperPlane [41] observes that I/O stacks in cloud data centers frequently resort to spin polling the many descriptor queues provided by modern NIC hardware, and proposes a new QWAIT hardware instruction which leverages the

processor’s cache mechanism (much like MWAIT) to watch many different in-memory descriptor queues at once, providing hardware acceleration for `select()` or `epoll()`-like operations. Evaluation is performed using the Gem5 simulator, although this implementation is not available. We take a different approach based on transferring data directly in cache lines without descriptors.

7.4 Exploring PIO

Neugebauer et. al. [44] provide a comprehensive analysis of PCIe performance in the context of NICs. The space where PIO is preferable to DMA for PCIe has been explored before. The hXDP [11] FPGA NIC work highlighted the high overhead of small PCIe transactions, and consequently performs small batch computations solely on the CPU.

In kPIO+WC [36] the authors demonstrate the benefit of write combining for PCIe-based PIO. Compared to a traditional DMA NIC, their FPGA-based prototype shows better latency and throughput for small and medium-sized messages and comparable throughput for large messages. The ThunderX-1 automatically performs combining for PCIe writes, and the results of Section 6.2 thus reflect this optimization.

Dagger [37] builds on CCI-P, the commercialized implementation of HARP’s coherent cache, to construct an FPGA-based NIC specialized for low latency RPC. A host-coherent cache holds connection states and the necessary structures for the transport layer on the NIC, while the payload remains in host memory. This minimizes FPGA memory demands, and exploits the lower latency of cache misses compared to conventional PCIe-based NICs..

8 Conclusion and Future Work

In this paper we have demonstrated that PIO on modern hardware outperforms DMA over a wide range of payload sizes in a number of different applications. For anything up to a disk block, VM page, or Ethernet Jumbo Frame, PIO offers (often dramatically) lower transfer times mostly thanks to its low fixed overheads. This advantage is consistent across RPC workloads, NIC packet transfer, and FPGA offloaded applications.

This strongly contradicts the accepted wisdom, under which these specific payloads and applications are the canonical examples of DMA-suitable tasks. Moving beyond conventional interconnects (PCIe), we have shown that the advantage grows even greater for the emerging class of coherent interconnects. This is partly due to a more suitably-sized unit of transfer (the cache line) and partly due to the opportunity to interact with the coherence protocol in a carefully-optimized manner.

Moving back to PIO makes sense in a landscape of plentiful, cheap CPU cores and fine-grained RPC-style workloads.

This work is ongoing, and we intend to develop it further in several ways. Both the cache-coherent NIC and Timely Dataflow offload designs will continue to be optimized, to explore the limits of PIO-style device communication on emerging coherent interconnects. We will also further explore the design of appropriate programming interfaces and OS-level integration of coherent mechanisms for high-performance devices.

References

- [1] Hakan Akkan, Michael Lang, and Lorie M. Liebrock. 2012. Stepping towards noiseless Linux environment. In *Proceedings of the 2nd International Workshop on Runtime and Operating Systems for Supercomputers*. ACM, Venice Italy, 1–7. <https://doi.org/10.1145/2318916.2318925>
- [2] Brian Allison, Michael Siegel, and Rick Hagen. 2020. OpenCAPI Transaction Layer Specification. (2020). <https://computeexpresslink.org/resource/opencvapi-specification-archive/>
- [3] Johnathan Alsop, Weon Taek Na, Matthew D. Sinclair, Samuel Grayson, and Sarita Adve. 2022. A Case for Fine-grain Coherence Specialization in Heterogeneous Systems. *ACM Trans. Archit. Code Optim.* 19, 3, Article 41 (aug 2022), 26 pages. <https://doi.org/10.1145/3530819>
- [4] Johnathan Alsop, Matthew D. Sinclair, and Sarita V. Adve. 2018. Spandex: a flexible interface for efficient heterogeneous coherence. In *Proceedings of the 45th Annual International Symposium on Computer Architecture* (Los Angeles, California) (ISCA '18). IEEE Press, 261–274. <https://doi.org/10.1109/ISCA.2018.00031>
- [5] AMBA® CHI Architecture Specification 2024. <https://developer.arm.com/documentation/ih0050/latest/>
- [6] Andrew Baumann, Paul Barham, Pierre-Evariste Dagand, Tim Harris, Rebecca Isaacs, Simon Peter, Timothy Roscoe, Adrian Schüpbach, and Akhilesh Singhanian. 2009. The Multikernel: A New OS Architecture for Scalable Multicore Systems. In *Proceedings of the ACM SIGOPS 22Nd Symposium on Operating Systems Principles* (Big Sky, Montana, USA) (SOSP '09). ACM, New York, NY, USA, 29–44. <https://doi.org/10.1145/1629575.1629579>
- [7] Andrew Bean. 2016. Improving memory access performance for irregular algorithms in heterogeneous CPU/FPGA systems. (Jan. 2016). <https://doi.org/10.25560/41981> Accepted: 2016-10-25T15:31:13Z Publisher: Imperial College London.
- [8] Berkeley Architecture Research. 2022. TileLink. <https://bar.eecs.berkeley.edu/projects/tilelink.html>
- [9] Burton H. Bloom. 1970. Space/time trade-offs in hash coding with allowable errors. *Commun. ACM* 13, 7 (July 1970), 422–426. <https://doi.org/10.1145/362686.362692>
- [10] Amirali Boroumand, Saugata Ghose, Minesh Patel, Hasan Hassan, Brandon Lucia, Rachata Ausavarungnirun, Kevin Hsieh, Nastaran Hajinazar, Krishna T. Malladi, Hongzhong Zheng, and Onur Mutlu. 2019. CoNDA: efficient cache coherence support for near-data accelerators. In *Proceedings of the 46th International Symposium on Computer Architecture* (ISCA '19). Association for Computing Machinery, New York, NY, USA, 629–642. <https://doi.org/10.1145/3307650.3322266>
- [11] Marco Spaziani Brunella, Giacomo Belocchi, Marco Bonola, Salvatore Pontarelli, Giuseppe Siracusano, Giuseppe Bianchi, Aniello Cammarano, Alessandro Palumbo, Luca Petrucci, and Roberto Bifulco. 2020. hXDP: Efficient Software Packet Processing on FPGA NICs. In *14th USENIX Symposium on Operating Systems Design and Implementation* (OSDI 20). USENIX Association, 973–990. <https://www.usenix.org/conference/osdi20/presentation/brunella>
- [12] CCIX Consortium and others. 2024. Cache Coherent Interconnect for Accelerators (CCIX). <http://www.ccixconsortium.com>
- [13] Mahesh Chaudhari, Kedar Kulkarni, Shreeya Badhe, and Vandana Inamdar. 2017. Evaluating Effect of Write Combining on PCIe Throughput to Improve HPC Interconnect Performance. In *2017 IEEE International Conference on Cluster Computing (CLUSTER)*. IEEE, Honolulu, HI, USA, 639–640. <https://doi.org/10.1109/CLUSTER.2017.109>
- [14] Shengsun Cho, Amoghavarsha Suresh, Tapti Palit, Michael Ferdman, and Nima Honarmand. 2018. Taming the killer microsecond. In *Proceedings of the 51st Annual IEEE/ACM International Symposium on Microarchitecture* (Fukuoka, Japan) (MICRO-51). IEEE Press, 627–640. <https://doi.org/10.1109/MICRO.2018.00057>
- [15] David Cock, Abishek Ramdas, Daniel Schwyn, Michael Giardino, Adam Turowski, Zhenhao He, Nora Hossle, Dario Korolija, Melissa Licciardello, Kristina Martsenko, Reto Achermann, Gustavo Alonso, and Timothy Roscoe. 2022. Enzian: an open, general CPU/FPGA platform for systems software research. In *Proceedings of the 27th ACM International Conference on Architectural Support for Programming Languages and Operating Systems* (Lausanne, Switzerland) (ASPLOS 2022). Association for Computing Machinery, New York, NY, USA, 590–607. <https://doi.org/10.1145/3503222.3507742>
- [16] SpinalHDL contributors. 2024. SpinalHDL. <https://github.com/SpinalHDL/SpinalHDL>.
- [17] Henry Cook, Wesley Terpstra, and Yunsup Lee. 2017. Diplomatic Design Patterns: A TileLink Case Study. In *First Workshop on Computer Architecture Research with RISC-V (CARRV 2017)*.
- [18] CXL Consortium. 2024. Compute Express Link. <https://www.computeexpresslink.org/>
- [19] Geetanjali Gadre, Shreeya Badhe, and Kedar Kulkarni. 2016. Network processor—A simplified approach for transport layer offloading on NIC. In *2016 International Conference on Advances in Computing, Communications and Informatics (ICACCI)*. IEEE, Jaipur, India, 2542–2548. <https://doi.org/10.1109/ICACCI.2016.7732440>
- [20] John Giacomoni, Tipp Moseley, and Manish Vachharajani. 2008. Fast-Forward for Efficient Pipeline Parallelism: A Cache-Optimized Concurrent Lock-Free Queue. In *Proceedings of the 13th ACM SIGPLAN Symposium on Principles and Practice of Parallel Programming* (Salt Lake City, UT, USA) (PPoPP '08). Association for Computing Machinery, New York, NY, USA, 43–52. <https://doi.org/10.1145/1345206.1345215>
- [21] Dan Gibson, Hema Hariharan, Eric Lance, Moray McLaren, Behnam Montazeri, Arjun Singh, Stephen Wang, Hassan M. G. Wassel, Zhehua Wu, Sunghwan Yoo, Raghuraman Balasubramanian, Prashant Chandra, Michael Cutforth, Peter Cuy, David Decotigny, Rakesh Gautam, Alex Iriza, Milo M. K. Martin, Rick Roy, Zuowei Shen, Ming Tan, Ye Tang, Monica Wong-Chan, Joe Zbiciak, and Amin Vahdat. 2022. Aquila: A unified, low-latency fabric for datacenter networks. 1249–1266. <https://www.usenix.org/conference/nsdi22/presentation/gibson>
- [22] Roberto Gioiosa, Thomas Warfel, Antonino Tumeo, and Ryan Friese. 2017. Pushing the Limits of Irregular Access Patterns on Emerging Network Architecture: A Case Study. In *2017 IEEE International Conference on Cluster Computing (CLUSTER)*. IEEE, Honolulu, HI, USA, 874–881. <https://doi.org/10.1109/CLUSTER.2017.125>
- [23] Mark Handley, Costin Raiciu, Alexandru Agache, Andrei Voinescu, Andrew W. Moore, Gianni Antichi, and Marcin Wójcik. 2017. Researching datacenter networks and stacks for low latency and high performance. In *Proceedings of the Conference of the ACM Special Interest Group on Data Communication*. ACM, Los Angeles CA USA, 29–42. <https://doi.org/10.1145/3098822.3098825>
- [24] Sara Hooker. 2021. The hardware lottery. *Commun. ACM* 64, 12 (Dec. 2021), 58–65. <https://doi.org/10.1145/3467017>
- [25] Wentao Hou, Jie Zhang, Zeke Wang, and Ming Liu. 2024. Understanding Routable PCIe Performance for Composable Infrastructures. In *21st USENIX Symposium on Networked Systems Design and Implementation (NSDI 24)*. USENIX Association, Santa Clara, CA, 297–312. <https://www.usenix.org/conference/nsdi24/presentation/hou>

- [26] Jack Tigar Humphries, Neel Natu, Kostis Kaffes, Stanko Novaković, Paul Turner, Hank Levy, David Culler, and Christos Kozyrakis. 2024. Tide: A Split OS Architecture for Control Plane Offloading. <http://arxiv.org/abs/2408.17351>
- [27] Intel. 2024. Intel Acceleration Stack for Intel® Xeon® CPU with FPGAs Core Cache Interface (CCI-P). <https://www.intel.com/content/www/us/en/docs/programmable/683193/current/acceleration-stack-for-cpu-with-fpgas.html>
- [28] Intel. 2024. Intel® Data Streaming Accelerator User Guide. (July 2024). <https://www.intel.com/content/www/us/en/content-details/759709/intel-data-streaming-accelerator-user-guide.html>
- [29] Intel Harp. 2024. IvyTown Xeon + FPGA: The HARP Program. https://cpufpga.wordpress.com/wp-content/uploads/2016/04/harp_isca_2016_final.pdf
- [30] Rishabh Iyer, Musa Unal, Marios Kogias, and George Candea. 2023. Achieving Microsecond-Scale Tail Latency Efficiently with Approximate Optimal Scheduling. In *Proceedings of the 29th Symposium on Operating Systems Principles (SOSP '23)*. Association for Computing Machinery, New York, NY, USA, 466–481. <https://doi.org/10.1145/3600066.3613136>
- [31] Christoforos Kachris, Konstantinos Kanonakis, and Ioannis Tomkos. 2013. Optical interconnection networks in data centers: recent trends and future challenges. *IEEE Communications Magazine* 51, 9 (Sept. 2013), 39–45. <https://doi.org/10.1109/MCOM.2013.6588648>
- [32] Kostis Kaffes, Timothy Chong, Jack Tigar Humphries, Adam Belay, David Mazières, and Christos Kozyrakis. 2019. Shinjuku: Preemptive Scheduling for msec-scale Tail Latency. In *16th USENIX Symposium on Networked Systems Design and Implementation (NSDI 19)*. USENIX Association, Boston, MA, 345–360. <https://www.usenix.org/conference/nsdi19/presentation/kaffes>
- [33] Sagar Karandikar, Chris Leary, Chris Kennelly, Jerry Zhao, Dinesh Parimi, Borivoje Nikolic, Krste Asanovic, and Parthasarathy Ranganathan. 2021. A Hardware Accelerator for Protocol Buffers. In *MICRO-54: 54th Annual IEEE/ACM International Symposium on Microarchitecture (Virtual Event, Greece) (MICRO '21)*. Association for Computing Machinery, New York, NY, USA, 462–478. <https://doi.org/10.1145/3466752.3480051>
- [34] Tomoya Kashimata, Toshiaki Kitamura, Keiji Kimura, and Hironori Kasahara. 2019. Cascaded DMA Controller for Speedup of Indirect Memory Access in Irregular Applications. In *2019 IEEE/ACM 9th Workshop on Irregular Applications: Architectures and Algorithms (IA3)*. IEEE, Denver, CO, USA, 71–76. <https://doi.org/10.1109/IA349570.2019.00017>
- [35] Kimberly Keeton. 2015. The Machine: An Architecture for Memory-centric Computing. In *Proceedings of the 5th International Workshop on Runtime and Operating Systems for Supercomputers*. ACM, Portland OR USA, 1–1. <https://doi.org/10.1145/2768405.2768406>
- [36] Steen Larsen and Ben Lee. 2015. Reevaluation of programmed I/O with write-combining buffers to improve I/O performance on cluster systems. In *2015 IEEE International Conference on Networking, Architecture and Storage (NAS)*. IEEE, Boston, MA, USA, 345–346. <https://doi.org/10.1109/NAS.2015.7255219>
- [37] Nikita Lazarev, Shaojie Xiang, Neil Adit, Zhiru Zhang, and Christina Delimitrou. 2021. Dagger: efficient and fast RPCs in cloud microservices with near-memory reconfigurable NICs. In *Proceedings of the 26th ACM International Conference on Architectural Support for Programming Languages and Operating Systems (Virtual, USA) (ASPLOS '21)*. Association for Computing Machinery, New York, NY, USA, 36–51. <https://doi.org/10.1145/3445814.3446696>
- [38] Huaicheng Li, Daniel S. Berger, Lisa Hsu, Daniel Ernst, Pantea Zardoshti, Stanko Novakovic, Monish Shah, Samir Rajadnya, Scott Lee, Ishwar Agarwal, Mark D. Hill, Marcus Fontoura, and Ricardo Bianchini. 2023. Pond: CXL-Based Memory Pooling Systems for Cloud Platforms. In *Proceedings of the 28th ACM International Conference on Architectural Support for Programming Languages and Operating Systems, Volume 2 (Vancouver, BC, Canada) (ASPLOS 2023)*. Association for Computing Machinery, New York, NY, USA, 574–587. <https://doi.org/10.1145/3575693.3578835>
- [39] Michael Marty, Marc de Kruijf, Jacob Adriaens, Christopher Alfeld, Sean Bauer, Carlo Contavalli, Michael Dalton, Nandita Dukkkipati, William C. Evans, Steve Gribble, Nicholas Kidd, Roman Kononov, Gautam Kumar, Carl Mauer, Emily Musick, Lena Olson, Erik Rubow, Michael Ryan, Kevin Springborn, Paul Turner, Valas Valancius, Xi Wang, and Amin Vahdat. 2019. Snap: a microkernel approach to host networking. In *Proceedings of the 27th ACM Symposium on Operating Systems Principles (Huntsville, Ontario, Canada) (SOSP '19)*. Association for Computing Machinery, New York, NY, USA, 399–413. <https://doi.org/10.1145/3341301.3359657>
- [40] Frank McSherry, Derek Gordon Murray, Rebecca Isaacs, and Michael Isard. 2013. Differential Dataflow. In *Conference on Innovative Data Systems Research*. <https://api.semanticscholar.org/CorpusID:18593675>
- [41] Amirhossein Mirhosseini, Hossein Golestani, and Thomas F. Wenisch. 2020. HyperPlane: A Scalable Low-Latency Notification Accelerator for Software Data Planes. In *2020 53rd Annual IEEE/ACM International Symposium on Microarchitecture (MICRO)*. 852–867. <https://doi.org/10.1109/MICRO50266.2020.00074>
- [42] Derek G. Murray, Frank McSherry, Rebecca Isaacs, Michael Isard, Paul Barham, and Martin Abadi. 2013. Naiad: a timely dataflow system. In *Proceedings of the Twenty-Fourth ACM Symposium on Operating Systems Principles (SOSP '13)*. Association for Computing Machinery, New York, NY, USA, 439–455. <https://doi.org/10.1145/2517349.2522738>
- [43] Vijay Nagarajan, Daniel J. Sorin, Mark D. Hill, and David A. Wood. 2020. *A Primer on Memory Consistency and Cache Coherence*. Springer International Publishing, Cham. <https://doi.org/10.1007/978-3-031-01764-3>
- [44] Rolf Neugebauer, Gianni Antichi, José Fernando Zazo, Yury Audzevich, Sergio López-Buedo, and Andrew W. Moore. 2018. Understanding PCIe performance for end host networking. In *Proceedings of the 2018 Conference of the ACM Special Interest Group on Data Communication (Budapest, Hungary) (SIGCOMM '18)*. Association for Computing Machinery, New York, NY, USA, 327–341. <https://doi.org/10.1145/3230543.3230560>
- [45] NVIDIA. 2024. NVLink. <https://www.nvidia.com/en-us/data-center/nvlink/>
- [46] Muhsen Owaida, David Sidler, Kaan Kara, and Gustavo Alonso. 2017. Centaur: A Framework for Hybrid CPU-FPGA Databases. In *2017 IEEE 25th Annual International Symposium on Field-Programmable Custom Computing Machines (FCCM)*. 211–218. <https://doi.org/10.1109/FCCM.2017.37>
- [47] Abishek Ramdas. 2023. *CCKit: FPGA acceleration in symmetric coherent heterogeneous platforms*. Doctoral Thesis. ETH Zurich. <https://doi.org/10.3929/ethz-b-000642567>
- [48] Hugo Sadok, Nirav Atre, Zhipeng Zhao, Daniel S. Berger, James C. Hoe, Aurojit Panda, Justine Sherry, and Ren Wang. 2023. Ensō: A Streaming Interface for NIC-Application Communication. In *17th USENIX Symposium on Operating Systems Design and Implementation (OSDI 23)*. USENIX Association, Boston, MA, 1005–1025. <https://www.usenix.org/conference/osdi23/presentation/sadok>
- [49] Henry N. Schuh, Arvind Krishnamurthy, David Culler, Henry M. Levy, Luigi Rizzo, Samira Khan, and Brent E. Stephens. 2024. CC-NIC: a Cache-Coherent Interface to the NIC. In *Proceedings of the 29th ACM International Conference on Architectural Support for Programming Languages and Operating Systems, Volume 1 (La Jolla, CA, USA) (ASPLOS '24)*. Association for Computing Machinery, New York, NY, USA, 52–68. <https://doi.org/10.1145/3617232.3624868>
- [50] Matthew D. Sinclair, Johnathan Alsop, and Sarita V. Adve. 2015. Efficient GPU synchronization without scopes: Saying no to complex consistency models. In *2015 48th Annual IEEE/ACM International Symposium on Microarchitecture (MICRO)*. 647–659. <https://doi.org/10.1145/2768405.2768406>

[//doi.org/10.1145/2830772.2830821](https://doi.org/10.1145/2830772.2830821)

- [51] J. Stuecheli, W. J. Starke, J. D. Irish, L. B. Arimilli, D. Dreps, B. Blaner, C. Wollbrink, and B. Allison. 2018. IBM POWER9 opens up a new era of acceleration enablement: OpenCAPI. *IBM Journal of Research and Development* 62, 4/5 (2018), 8:1–8:8. <https://doi.org/10.1147/JRD.2018.2856978>
- [52] Sajjad Tamimi, Florian Stock, Andreas Koch, Arthur Bernhardt, and Iliia Petrov. 2022. An Evaluation of Using CCIX for Cache-Coherent Host-FPGA Interfacing. In *2022 IEEE 30th Annual International Symposium on Field-Programmable Custom Computing Machines (FCCM)*, 1–9. <https://doi.org/10.1109/FCCM53951.2022.9786103>
- [53] Wesley W Terpstra. 2017. TileLink: A free and open-source, high-performance scalable cache-coherent fabric designed for RISC-V. In *Proc. 7th RISC-V Workshop*.
- [54] James Thomas, Pat Hanrahan, and Matei Zaharia. 2020. Fleet: A Framework for Massively Parallel Streaming on FPGAs. In *Proceedings of the Twenty-Fifth International Conference on Architectural Support for Programming Languages and Operating Systems*. ACM, Lausanne Switzerland, 639–651. <https://doi.org/10.1145/3373376.3378495>
- [55] Tianrui Wei, Nazerke Turtayeva, Marcelo Orenes-Vera, Omkar Lonkar, and Jonathan Balkind. 2023. Cohort: Software-Oriented Acceleration for Heterogeneous SoCs. In *Proceedings of the 28th ACM International Conference on Architectural Support for Programming Languages and Operating Systems, Volume 3 (ASPLOS 2023)*. Association for Computing Machinery, New York, NY, USA, 105–117. <https://doi.org/10.1145/3582016.3582059>
- [56] Ying Wei, Yi Chieh Huang, Haiming Tang, Nithya Sankaran, Ish Chadha, Dai Dai, Olakanmi Oluwole, Vishnu Balan, and Edward Lee. 2023. 9.3 NVLink-C2C: A Coherent Off Package Chip-to-Chip Interconnect with 40Gbps/pin Single-ended Signaling. In *2023 IEEE International Solid-State Circuits Conference (ISSCC)*, 160–162. <https://doi.org/10.1109/ISSCC42615.2023.10067395>
- [57] Xilinx DMA Benchmark 2024. https://github.com/Xilinx/dma_ip_drivers/tree/master
- [58] Hanqing Zeng and Viktor Prasanna. 2020. GraphACT: Accelerating GCN Training on CPU-FPGA Heterogeneous Platforms. In *Proceedings of the 2020 ACM/SIGDA International Symposium on Field-Programmable Gate Arrays*. ACM, Seaside CA USA, 255–265. <https://doi.org/10.1145/3373087.3375312>